

---

# Minimum Cost Active Labeling

---

**Hang Qiu**  
USC  
hangqiu@usc.edu

**Krishna Chintalapudi**  
Microsoft Research  
krchinta@microsoft.com

**Ramesh Govindan**  
USC  
ramesh@usc.edu

## Abstract

Labeling a data set completely is important for groundtruth generation. In this paper, we consider the problem of *minimum-cost* labeling: classifying all images in a large data set with a target accuracy bound at minimum dollar cost. Human labeling can be prohibitive, so we train a classifier to accurately label part of the data set. However, training the classifier can be expensive too, particularly with active learning. Our min-cost labeling uses a variant of active learning to learn a model to predict the optimal training set size for the classifier that minimizes *overall cost*, then uses active learning to train the classifier to maximize the number of samples the classifier can correctly label. We validate our approach on well known public data sets such as Fashion, CIFAR-10 and CIFAR-100. In some cases, our approach has  $6\times$  lower overall cost relative to human labeling, and is always cheaper than the cheapest active learning strategy.

## 1 Introduction

Groundtruth data is crucial for training and testing ML models. Today, labeling services [1, 3, 2] typically employ humans to generate groundtruth, which can incur significant cost. A cheaper alternative is to train a classifier using human generated labels for a subset of the data, then generate labels using this classifier at almost negligible cost for the rest of the data. There are two key challenges with this approach. First, the accuracy of the labels generated by the classifier may be less than that of human labeling. Second, the cost (in \$) of training the classifier itself can become significant and potentially offset the gains obtained from avoiding human labeling. In this paper we ask the question: “How can we minimize the overall cost of generating groundtruth (in \$ including training and human labeling costs) for an unlabeled data set  $X$ , while ensuring that the overall error rate of the generated groundtruth is less than  $\epsilon$  (e.g., 5%), assuming human generated labels as the gold standard?”

Suppose that a classifier  $\mathcal{D}(B)$  is trained using human generated labels for  $B \subset X$ . Let the error rate of  $\mathcal{D}(B)$  over the remaining unlabeled data using  $\mathcal{D}(B)$  be  $\epsilon(X \setminus B)$ . If  $\mathcal{D}(B)$  were used to generate labels for this remaining data, the overall groundtruth error rate for  $X$  would be,  $\epsilon(X) = (1 - |B|/|X|)\epsilon(X \setminus B)$  (0% for  $B$ , because we have assumed human labeling is perfect). If  $\epsilon(X) \geq \epsilon$ , then, this would violate the maximum error rate requirement.

However,  $\mathcal{D}(B)$  might still be able to generate accurate labels for a carefully chosen subset  $S(\mathcal{D}, B) \subset X \setminus B$  (e.g., comprising only those that  $\mathcal{D}(B)$  is very confident about). After generating labels for  $S(\mathcal{D}, B)$  using  $\mathcal{D}(B)$ , labels for the remaining  $X \setminus B \setminus S(\mathcal{D}, B)$  can be once again generated by humans. The *overall error rate* of the generated groundtruth then would be,  $(|S(\mathcal{D}, B)|/|X|)\epsilon(S(\mathcal{D}, B)) + \epsilon(X \setminus B \setminus S(\mathcal{D}, B))$ .  $\epsilon(S(\mathcal{D}, B))$  is the error rate of generating labels over  $S(\mathcal{D}, B)$  using  $\mathcal{D}(B)$  and is, in general, higher for larger  $|S(\mathcal{D}, B)|$ . Let  $S^*(\mathcal{D}, B)$  be the largest possible  $S(\mathcal{D}, B)$  that ensures that the overall error rate is less than  $\epsilon$ . Then, overall cost of generating labels in this manner is:

$$C = (|X \setminus S^*(\mathcal{D}, B)|) \cdot C_h + C_t(\mathcal{D}(B)) \quad (1)$$

where,  $C_h$  is the cost of human labeling for a single data item and  $C_t(\mathcal{D}(B))$  is the total cost of generating  $\mathcal{D}(B)$  including the cost of finding  $B$  and training  $\mathcal{D}(B)$  but not including the human labeling cost  $|B| C_h$ .

The key contribution in this paper is *min-cost active labeling* (MCAL), an active learning [29] based approach that minimizes  $\mathbf{C}$  as follows:

$$\begin{aligned} \mathbf{C}^* = \operatorname{argmin}_{S^*(\mathcal{D}, B), B} \mathbf{C} \\ \text{subject to } (|S^*(\mathcal{D}, B)|)/(|X|)\epsilon(S^*(\mathcal{D}, B)) < \epsilon \end{aligned}$$

MCAL follows a similar iterative process as active learning when generating  $B$ . In each iteration, it ranks data  $X \setminus B$  using a function  $M(\cdot)$  that measures their “informativeness”, based on  $\mathcal{D}(B)$ ’s classification uncertainty (e.g., entropy [12] or margin [29]). MCAL then obtains human labels for the  $\delta$  (batch size) most informative ones, adds them to  $B$ , and (repeatedly) re-trains  $\mathcal{D}$  using  $B$ .

However, MCAL differs from active learning in one crucial aspect. Unlike standard active learning which aims to minimize  $|B|$  while achieving a high accuracy for  $\mathcal{D}$ , MCAL optimizes  $\mathbf{C}$  by *jointly selecting*  $S^*(\mathcal{D}, B)$  and  $B$ . As  $|B|$  increases,  $\mathcal{D}(B)$ ’s prediction accuracy improves. However, this accuracy has a *concave* relationship with  $|B|$ : more and more data must be human labeled for incremental improvements in  $\mathcal{D}$ ’s accuracy. On the other hand, the cost of training  $\mathcal{D}$  using active learning,  $C_t(\mathcal{D}(B))$ , typically has a *convex* dependency on  $|B|$ , making it more and more expensive to train over larger  $B$  and it also accumulates across active learning iterations (§3). Both these dependencies make it harder to improve  $\mathcal{D}$ ’s accuracy per unit cost (in \$) as  $|B|$  increases. Thus, continuing to perform active learning becomes counter-productive beyond a certain point.

This dependency of  $\mathbf{C}$  on  $|B|$  is data set specific. Thus, a key challenge for MCAL is that it must model and predict  $\mathbf{C}$  as a function of  $|B|$  during active learning. Using this model, then it must jointly: i) decide when to terminate active learning, ii) adapt  $\delta$  to limit training costs while not degrading the active learning efficiency, and iii) select an appropriate  $S^*(\mathcal{D}, B)$ . To this end, this paper makes the following contributions:

- It develops a method to construct, and iteratively refine, a model for predicting  $\mathbf{C}$  as a function of  $|B|$  and a procedure to find  $S^*(\mathcal{D}, B)$ . (§3).
- It presents the MCAL algorithm (§4) that terminates active learning when it is counter-productive to add human-generated labels into  $|B|$ . In effect, this is the point at which the total cost (Equation 1) is minimized. MCAL can also select, from a small set of network architectures for  $\mathcal{D}$ , the one that achieves lowest-cost labeling.
- Evaluations (§5) of MCAL on various popular benchmark datasets of different levels of difficulty (Fashion-MNIST [33], CIFAR-10 [24] and CIFAR-100 [24]) show that it achieves lower than the lowest-cost labeling achieved by an active learning strategy that trains a classifier to label the dataset. It selects a strategy that matches the complexity of the data set and the classification task. For example, it labels the Fashion dataset, the easiest to classify, using a trained classifier. At the other end, it chooses to label CIFAR-100 using humans almost completely; for this data set, it estimates training costs to be prohibitive. Finally, it labels a little over half of CIFAR-10 using a classifier. MCAL is up to  $6\times$  cheaper for some data sets compared to human labeling all images. It is able to achieve these savings, in part, by carefully determining active learning batch sizes while accounting for training costs; cost savings due to active learning range from 20-32% for Fashion and CIFAR-10.

## 2 Related Work

To label large data sets, annotation platforms such as Amazon SageMaker [1], Figure Eight [2], and Google Labeling Services [3], rely on humans. Annotation by human experts can be expensive, and Amazon Sagemaker allows users to trade-off annotation quality for a lower cost. MCAL is motivated by this, and attempts to lower cost without compromising quality.

Active learning [29] aims to reduce labeling cost in training a model, by iteratively selecting the most informative samples for labeling. Early work focused on designing metrics for sample selection based on margin sampling [29], max entropy [12] and least confidence [11]. Recent work has focused

on developing metrics tailored to specific tasks, such as classification [28], detection [7, 19], and segmentation [21, 34], or for specialized settings such as when costs depend upon the label [23], or for a hierarchy of labels [16]. Other work in this area has explored variants of the problem of sample selection: leveraging model structure [32], using model ensembles to improve sampling efficacy [6], or using self-supervised mining of samples for active learning to avoid data set skew [31]. MCAL uses active learning for training the classifier  $D$  (§1) and can accommodate multiple sample selection metrics  $M(\cdot)$ .

More recent work has explored techniques to learn active learning strategies, using reinforcement learning [22] or one-shot meta-learning [10]. However, with the exception of [30] which designs a lightweight model to reduce the iterative training cost incurred in active learning, we have not found any work that takes training cost into account when developing an active learning strategy. Because active learning can incur significant training cost, MCAL includes training costs in its formulation.

Training cost figures prominently in the literature on hyper-parameter tuning, especially for architecture search. Prior work has attempted to predict learning curves to prune hyper-parameter search [20], develop techniques to find the most effective search strategy within a given budget [25], or build a model to characterize maximum achievable accuracy on a given dataset to enable fast triage during architecture search [17], all with the goal of reducing training cost.

Also relevant is the long line of work that has empirically observed a power-law relationship between generalization error and training set size [5, 15, 18, 27, 13, 9] across a wide variety of tasks and models. MCAL builds upon this observation, and learns the parameters of a truncated power-law model with as few samples as possible using active learning, which it uses to learn  $B$ .

### 3 Prediction Models for C

MCAL must determine the optimal value of  $B$  and  $S^*(\mathcal{D}, B)$  that minimizes  $C$  (§1). Thus, in order to make optimal choices for various parameters then, MCAL must be able to predict  $C$  as a function of the choices.  $C$  in turn depends on  $|S^*(\mathcal{D}, B)|$  and  $C_t(\mathcal{D}(B))$  (Equation 1). Thus, MCAL actually constructs two predictors, one each for  $|S^*(\mathcal{D}, B)|$  and  $C_t(\mathcal{D}(B))$ .

#### 3.1 Predicting $|S^*(\mathcal{D}, B)|$ as a function of $|B|$

After training the classifier  $\mathcal{D}$  on the human labeled data  $B$  generated thus far, MCAL sorts each unlabeled data item in  $X \setminus B$  using  $M(\cdot)$ , a measure of the item’s informativeness. Let the set  $S^\theta(\mathcal{D}(B))$  contain the  $\theta \cdot |X \setminus B|$  least informative data items ( $\theta \in (0, 1)$ ); these are the items that  $\mathcal{D}$  is most confident about. Thus,  $S^*(\mathcal{D}, B)$  corresponds to an  $S^\theta(\mathcal{D}(B))$  for a maximal value  $\theta^*$  that does not violate the overall groundtruth accuracy constraint  $(|S^*(\mathcal{D}, B)|)/(|X|)\epsilon(S(\mathcal{D}, B)) < \epsilon$ . MCAL constructs a predictor for  $\epsilon(S^\theta(\mathcal{D}(B)))$  and uses it to predict  $|S^*(\mathcal{D}, B)|$  by searching for  $\theta^*$ .

To predict  $\epsilon(S^\theta(\mathcal{D}(B)))$ , we leverage recent empirical work (§2) that observes that, for many tasks and many models, the generalization error vs. training set size is well-modeled by a power-law [15, 18, 27, 13, 9] of the form  $\epsilon(S^\theta(\mathcal{D}(B))) = \alpha_\theta |B|^{-\gamma_\theta}$ . However, it is well-known that most power-laws experience a fall-off [8] at high values of the independent variable. To model this, we use an *upper-truncated* power-law [8]:

$$\epsilon(S^\theta(\mathcal{D}(B))) = \alpha_\theta |B|^{-\gamma_\theta} e^{-\frac{|B|}{k_\theta}} \quad (2)$$

This model better represents the generalization vs. training error relationship than a power-law, as Figure 1 illustrates (Appendix A demonstrates this for other datasets). In this figure, we use active learning on the CIFAR-10 [24] data set, trained using RESNET18 [14]. We fit both a power-law and a truncated power-law. As the figure shows, the truncated power-law is able to better predict the generalization error at larger values of  $|B|$ .

$\epsilon(S^\theta(\mathcal{D}(B)))$  is expected to increase monotonically with  $\theta$  as increasing  $\theta$  has the effect of adding data that  $\mathcal{D}$  is progressively less confident about. Lacking a parametric model for this dependence, to find  $\theta^*$ , we generate power-law models  $\epsilon(S^\theta(\mathcal{D}(B)))$  for various discrete values of  $\theta \in (0, 1)$  as described in §4.  $\theta^*$  for a given  $B$  is then predicted by searching across the predicted  $\epsilon(S^\theta(\mathcal{D}(B)))$  corresponding to the discrete values of  $\theta$ .

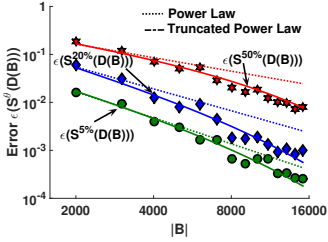


**Figure 1:** Power law and Truncated Power law fits on CIFAR-10 using RESNET18 for various  $\epsilon(S^\theta(\mathcal{D}(B)))$

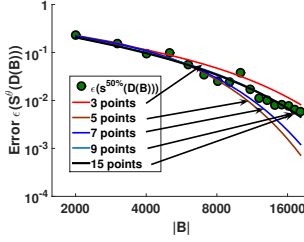


**Figure 2:** Power law fit for  $\epsilon(S^\theta(\mathcal{D}(B)))$  improves with increasing number of error estimates for CIFAR-10 using RESNET18.

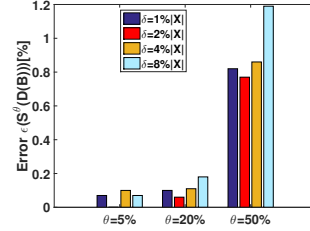


**Figure 3:** Dependence of  $\epsilon(S^\theta(\mathcal{D}(B)))$  on  $\delta$  is "small" especially towards the end of active learning. Here,  $(|B| = 16,000)$  for CIFAR-10 using RESNET18.

### 3.2 Modeling Active Learning Training Costs

Active learning [29] iteratively obtains human labels for  $\delta$  most informative items ranked using  $M(\cdot)$  and adds them to  $B$ . It then re-trains the classifier  $\mathcal{D}$  using the entire set  $B$ . A smaller  $\delta$  typically makes the active learning more effective: it allows for achieving a lower error for a potentially smaller  $B$  through more frequent sampling, but also significantly increases the training cost due to frequent re-training of  $\mathcal{D}$ . Choosing an appropriate  $\delta$  is thus an important aspect of minimizing overall cost.

The training cost (in \$) depends on the training time, which in turn is proportional to the data size  $(|B|)$  and the number of epochs used to train the model (each epoch running over the entire  $B$ ). A common strategy in active learning approaches is to use a fixed number of epochs per iteration, so the training cost in each iteration is proportional to the  $|B|$ . Since in each iteration  $\delta$  new data samples are added to  $B$ , the total training cost accumulated over all the previous and current iterations is:

$$C_t(\mathcal{D}(B)) = k |B| \left( \frac{|B|}{\delta} + 1 \right) \quad (3)$$

Figure 9, generated for CIFAR-10 on RESNET18, shows this quadratic dependence on  $|B|$  for different  $\delta$ . MCAL does not depend on the specific form of the training cost, so can accommodate other cost models (e.g., if the number of epochs is proportional to  $|B|$  in which case  $C_t(\mathcal{D}(B))$  can have a cubic dependency on  $|B|$ ).

While  $\epsilon(S^\theta(\mathcal{D}(B)))$  also depends on  $\delta$  in theory, in practice this dependence is insignificant relative to  $C_t(\mathcal{D}(B))$ . To illustrate this, Figure 3 depicts values of  $\epsilon(S^\theta(\mathcal{D}(B)))$  for various  $\theta$  for CIFAR-10 using RESNET18, across a range of values of  $\delta$ . This variation is less than 1% especially for smaller values of  $\theta$ .

## 4 The MCAL Algorithm

MCAL is described in Algorithm 1. It takes as input an active learning metric  $M(\cdot)$ , the specific classifier  $\mathcal{D}$  (e.g., RESNET18) and the parametric models for training cost (e.g., Eqn 3) and for error rate as a function of training size (e.g., the truncated power law in Eqn 2). At a high-level, the algorithm operates in two phases. In the first phase, it uses estimates obtained during active learning to learn the parameters of the truncated power-law model for various  $\theta$  and the cost measurements to learn the parameters for training cost model. In the second phase, having the models, it can estimate and refine  $S^*(\mathcal{D}, B)$  and  $B$  that produce the optimal cost  $\mathbf{C}^*$ . It can also estimate the optimal batch size  $\delta_{opt}$  for this cost. It terminates when adding more samples to  $B$  is counter productive. It trains a classifier to label  $S^*(\mathcal{D}, B)$  and generates human labels for the remaining unlabeled samples.

The first four steps perform initialization. The first step (Line 1) randomly selects a test set  $\mathbf{T}$  ( $|T| = 5\%$  of  $|X|$ ) and obtains human labels, so that it can be used to test and measure the performance of  $\mathcal{D}$ . Line 2 initializes  $B = B_0$  by randomly selecting  $\delta_0$  (1% of  $X$  in our implementation) samples from  $X$  and obtaining human labels for these. Line 3 trains  $\mathcal{D}$  using  $B_0$  and uses  $T$  to estimate the generalization errors  $\epsilon_T(S^\theta(\mathcal{D}(B_0)))$  for various values of  $\theta \in (0, 1)$  (we chose in increments of 0.05  $\{0.05, 0.1, \dots, 1\}$ ), using  $T$  and  $M(\cdot)$ .

---

**Algorithm 1** MCAL

---

**Inputs:** An active learning metric  $M(\cdot)$ , a classifier  $\mathcal{D}$ , set of unlabeled images ( $X$ ), a parametric model to predict  $C_t(\mathcal{D}(B))$  and a parametric model to predict  $\epsilon(S^\theta(\mathcal{D}(B)))$

- 1: Obtain human generated labels for a randomly sampled test set  $T \subset X$ , and let  $X = X \setminus T$ .
- 2: Obtain human generated labels for a randomly sampled data items  $B_0 \subset X$ ,  $|B_0| = \delta_0$ .
- 3: Train  $\mathcal{D}(B_0)$  and test the classifier over  $T$
- 4: Record training cost  $C_t(\mathcal{D}(B_0))$
- 5: **for**  $\theta \in \{\theta_{min}, \dots, \theta_{max}\}$  **do**
- 6:     Estimate  $\epsilon_T(S^\theta(\mathcal{D}(B_0)))$  using  $T$  and  $M(\cdot)$
- 7: **end for**
- 8: Initialization:  $\mathbf{C}_{new}^* = 0$ ,  $\mathbf{C}_{old}^* = 0$ ,  $\delta = \delta_0$ ,  $i = 1$ ,  $B_{opt} = B_0$
- 9: **while**  $\mathbf{C}^* < \mathbf{C}(B_{opt} + \delta)$  **do**
- 10:     Obtain human generated labels for  $b_i \subset X \setminus B_{i-1}$  comprising  $|b_i| = \delta$  most informative samples ranked using  $M(\cdot)$
- 11:      $B_i = B_{i-1} \cup b_i$
- 12:     Train  $\mathcal{D}(B_i)$  and test the classifier over  $T$
- 13:     Record  $C_t(\mathcal{D}(B_i))$ , and update parameters for  $C_t(\mathcal{D}(B))$  using  $\langle |B_k|, C_t(\mathcal{D}(B_k)) \rangle, \forall k$
- 14:     **for**  $\theta \in [\theta_{min}, \dots, \theta_{max}]$  **do**
- 15:         Estimate  $\epsilon_T(S^\theta(\mathcal{D}(B_i)))$  using  $T$  and  $M(\cdot)$
- 16:         Update the model parameters for  $\epsilon(S^\theta(\mathcal{D}(B)))$  using  $\langle |B_k|, \epsilon_T(S^\theta(\mathcal{D}(B_k))) \rangle, \forall k$
- 17:     **end for**
- 18:     Find  $\mathbf{C}_{new}^* = \mathbf{C}^*$ ,  $B_{opt}$  as described in Section 3
- 19:     **if**  $(|\mathbf{C}_{new}^* - \mathbf{C}_{old}^*|) / |\mathbf{C}_{new}^*| < \Delta$  **then**
- 20:          $\text{argmin}_N \delta_{opt} = (|B_{opt}| - |B_i|) / N$ , s.t.  $\mathbf{C} < \mathbf{C}^*(1 + \beta)$
- 21:          $\delta = \delta_{opt}$
- 22:     **end if**
- 23:      $\mathbf{C}_{old}^* = \mathbf{C}_{new}^*$
- 24:      $i = i + 1$
- 25: **end while**
- 26: Use  $\mathcal{D}(B_{opt})$  and  $M(\cdot)$  to find  $S^*(\mathcal{D}, B_{opt})$
- 27: Annotate the residual  $X \setminus B \setminus S^*(\mathcal{D}, B_{opt})$

---

After these initial steps, the main loop of min-cost active labeling begins (Line 9). In each step, as with standard active learning, MCAL selects  $\delta$  most informative samples  $M(\cdot)$ , obtains their labels and adds them to  $B$  (Line 11), then trains  $\mathcal{D}$  on them (Line 12). The primary difference with active learning is that MCAL, in every iteration, estimates the model parameters for  $\epsilon(S^\theta(\mathcal{D}(B)))$  and  $S^\theta(\mathcal{D}(B))$  (Line 13, 16), then uses these to estimate  $\mathbf{C}^*$  and  $B_{opt}$  (Line 18). At the end of this step, MCAL can answer the question: “How many human generated labels must be obtained into  $B$  to train  $\mathcal{D}$ , in order to minimize  $\mathbf{C}^*$ ” (§3).

The estimated model parameters for  $C_t(\mathcal{D}(B))$  and  $\epsilon(S^\theta(\mathcal{D}(B)))$  may not be stable in the first few iterations (in our experience, 3 when using the truncated power law) given limited data for the fit. To determine if the model parameters are stable, MCAL compares the estimated  $\mathbf{C}^*$  (in dollars) obtained from the previous iteration to the current. If the difference is small (within 5%, in our implementation), the model is considered to be stable enough for use (Line 19).

After the predictive models have stabilized, we can rely on the estimates of  $B_{opt}$ , the final number of labels to be obtained into  $B$ , and consequently the remaining number of samples needed  $B_{opt} \setminus B_i$ . At this point MCAL adjusts  $\delta$  (Line 21) to reduce the training cost when it is possible to do so. MCAL can do this because it targets relatively high accuracy for  $\mathcal{D}(B)$ . For these high targets, it is important to continue to improve model parameter estimates (*e.g.*, the parameters for the truncated power law), and active learning can help achieve this. Figure 2 shows how the fit to the truncated power law improves as more points are added. Finally, unlike active learning, MCAL adapts  $\delta$  to achieve lower training cost. Figure 3 shows that, for most values of  $\theta$ , the choice of  $\delta$  does not affect classifier accuracy significantly. While, the choice of active learning batch size does not affect the final classifier accuracy, but it can significantly impact training cost (§3).

This loop terminates when total cost obtained in a step is higher than that obtained in the previous step. At this point, MCAL simply trains the classifier using the last value of  $B_{opt}$ , then human labels any remaining unlabeled samples (Lines 26, 27).

**Extending MCAL to selecting the cheapest DNN architecture.** In what we have described so far, we have assumed that min-cost labeling is given a candidate DNN architecture for  $D$ . However, it is trivial to extend MCAL to the case when the data set curator supplies a small number  $m$  (typically 2-4) of candidate classifier architectures  $\{\mathcal{D}_1, \mathcal{D}_2, \dots\}$ . In this case, MCAL can generate separate prediction models for each of the classifiers and pick the one that minimizes  $\mathbf{C}$  once the model parameters have stabilized. This does not inflate the cost significantly since the training costs until this time are over small sizes of  $B$  and not significant.

## 5 Evaluation

In this section, we evaluate the performance of MCAL over three popular classification data sets: Fashion-MNIST [33], CIFAR-10 [24] and CIFAR-100 [24]. We chose these three data sets to demonstrate that MCAL can work effectively across classification tasks with different difficulty levels, Fashion-MNIST being the “easiest” and CIFAR-100 the “hardest”. We use three popular DNN architectures RESNET50, RESNET18 [14], and CNN18 (RESNET18 without the skip connections). These architectures span the range of architectural complexity with differing training costs and achievable accuracy. CNN18 has a very low training cost but yields lower accuracy while RESNET50 has a very high training cost and typically yields the highest accuracy. This allows us to demonstrate how MCAL can effectively select the most cost efficient architecture among available choices. We also use two different human labeling services: Amazon labeling services [1] at 0.04 USD/image and Satyam [26] at 0.003 USD/image. Satyam labels images  $10\times$  cheaper by leveraging untrained inexpensive workers. This allows to demonstrate how MCAL adapts to changing human labeling costs. Finally, our evaluation ignores model fitting and inference costs, since they are negligible compared to training costs.

MCAL uses a popular active learning metric (margin [29]) to rank and select samples for all our results in this section. At each active learning iteration, it trains the model over 200 epochs with a  $10\times$  learning rate reduction at 80, 120, 160, 180 epochs, and a mini-batch-size of 256 samples [4]. We have left it to future work to incorporate hyper-parameter search into the optimization.

DNN	CNN-18 <sup>†</sup>	RESNET18	RESNET50
Cost	0.00007	0.0003	0.0009

**Table 1:** Training Costs in USD Per Image for various DNN architectures

Table 1 depicts the training cost per image for three different DNNs trained on CIFAR-10. We use a virtual machine with 4 NVIDIA K80 GPUs at 3.6 USD/hr and maintain over 90% utilization on each GPU during the training process. In all experiments, unless otherwise specified, the overall labeling accuracy requirement  $\epsilon$  was set at 5%.

Data Set	Labeling Service	$\frac{ B }{ X }$	$\frac{ S }{ X }$	DNN Selected	Labeling Error	Human Cost (\$)	MCAL Cost (\$)
Fashion	Amazon	6.1%	85.0%	RESNET18	4.0%	2800	400
	Satyam	8.4%	85.0%	RESNET18	4.0%	210	29
CIFAR-10	Amazon	22.2%	65.0%	RESNET18	2.4%	2400	792
	Satyam	27.0%	65.0%	RESNET18	2.4%	180	63
CIFAR-100	Amazon	32.0%	10.0%	RESNET18	0.4%	2400	1698
	Satyam	57.6%	20.0%	RESNET18	1%	180	139

**Table 2:** Summary of results

### 5.1 Reduction in Labeling Costs

MCAL automatically makes three key decisions to minimize overall labeling cost. It a) selects the subset of images that the classifier should be trained on ( $|B|_{opt}$ ), b) adapts  $\delta$  across active learning iterations to keep training costs in check, and c) selects the best DNN architecture from among a set of candidates (CNN18, RESNET18 and RESNET50). In this section, we demonstrate that MCAL



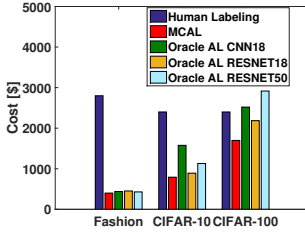


**Figure 4:** Total cost of labeling for various data sets, for i) Human labeling, ii) MCAL and iii) Oracle assisted AL for various DNN architectures.

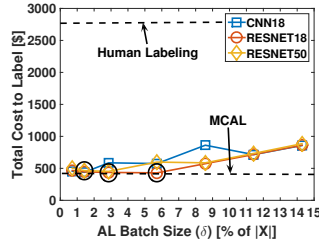


**Figure 5:** Dependence of overall cost of using naive active learning on  $\delta$  for Fashion using Amazon labeling service.

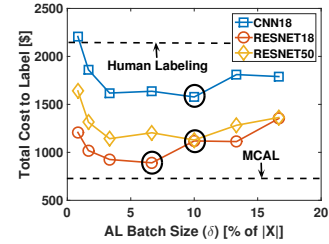


**Figure 6:** Dependence of overall cost of using naive active learning on  $\delta$  for CIFAR-10 using Amazon labeling service.

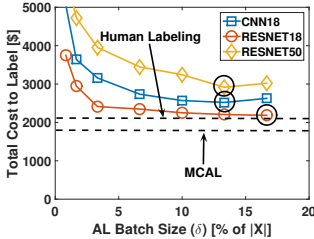


**Figure 7:** Dependence of overall cost of using naive active learning on  $\delta$  for CIFAR-100 using Amazon labeling service.

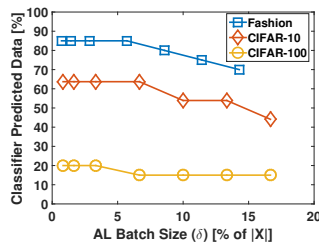


**Figure 8:** Dependence of  $\frac{|S^*(D(B))|}{|X|}$  for a fixed  $\delta$  using RESNET18.

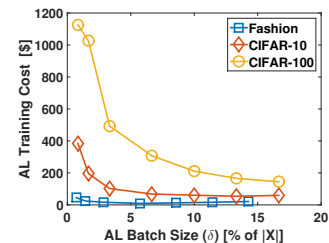


**Figure 9:** Active learning training cost (in \$) as a function of batch size ( $\delta$ ) using RESNET18.

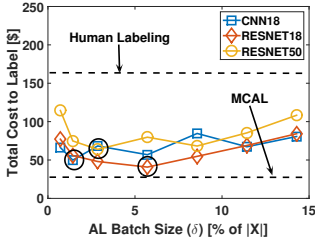
provides significant overall cost benefits at the expense of  $\epsilon$  (5%) degradation in label quality. Further, it outperforms active learning even when an oracle is used to choose the optimal  $\delta$ .

Figure 4 depicts the total labeling costs incurred when using Amazon labeling services for three different schemes: i) when humans are used to label the entire data set using Amazon labeling services, ii) MCAL for  $\epsilon = 5\%$ , and iii) active learning with an oracle to choose  $\delta$  for the DNN architectures CNN18, RESNET18 and RESNET50. Table 2 lists the numerical values of the costs (in \$) for human labeling and MCAL.

**Cost Saving Compared to Human Labeling.** From Figure 4 and Table 2, MCAL provides an overall cost saving of 86%, 67% and 30% for Fashion, CIFAR-10 and CIFAR-100 respectively. As expected, the savings depend on the “hardness” of the classification task. Table 2 also shows the number of samples in  $B$  used to train  $D$ , as well as the number of samples  $|S|$  labeled using  $D$ . For Fashion, MCAL labels only 6.1% of the data to train the classifier and uses it to label 85% of the data set. For CIFAR-10, it trains using 22% of the data set and labels about 65% of the data using the classifier. CIFAR-100 requires more data to train the classifier to a high accuracy so is able to label only 10% of the data using the classifier. Table 2 shows that MCAL, for each data set, is able to achieve the overall accuracy constraint of  $\epsilon < 5\%$ .

**Cost Savings Compared to Oracle-assisted Active Learning.** We experimentally determined the optimal  $\delta$  for active learning, for each data set and architecture combination; we call this *oracle-assisted active learning*. To do this, using various values of  $\delta$  between 1% to 20% of  $|X|$ , we ran active learning to label each dataset until the desired labeling error constraint was met. We then chose the  $\delta$  with the lowest overall cost. The dependence of overall cost on  $\delta$  for each of the DNNs and data set combinations can be seen in Figure 5, Figure 6, and Figure 7.

Figure 4 shows that MCAL is cheaper than even oracle-assisted active learning for all the three DNN choices. It achieves this by determining when to stop active learning for each data set, adapting the  $\delta$  and choosing the cheapest DNN architecture. It is interesting to note that oracle-assisted active



**Figure 10:** Performance of MCAL compared to naive active learning on Fashion using Satyam labeling

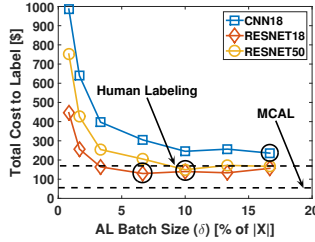


**Figure 11:** Performance of MCAL compared to naive active learning on CIFAR-10 using Satyam labeling

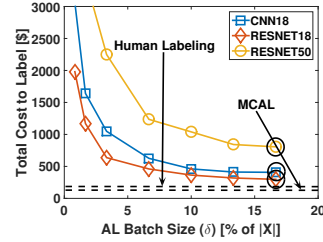


**Figure 12:** Performance of MCAL compared to naive active learning on CIFAR-100 using Satyam labeling

learning is more expensive than human labeling on CIFAR-100 when using CNN18 and RESNET50. This is because oracle-assisted active learning does not take training costs into account.

**Understanding the effect of  $\delta$ .** Figure 8 depicts the number of samples labeled using the classifier, for various choices of  $\delta$  for each of the data sets using RESNET18. As seen from Figure 8, while the number of classifier-labeled samples decreases with increasing  $\delta$ , the reduction is not significant until a certain point (*e.g.*, 7% for CIFAR-10 and Fashion). Training costs decrease as  $\frac{1}{\delta^2}$  as depicted in Figure 9. Thus, choosing a delta too small can be sub-optimal for overall cost. This is also seen in Figure 5, Figure 6, and Figure 7 which show (using a circle) the  $\delta$  with minimum overall cost.

**Summary.** Table 2 and Figures 4-9 show how MCAL is able to adapt to different kinds of data sets, classification tasks and DNN architectures and consistently minimize overall cost while providing the required labeling quality guarantees.

## 5.2 Effect of cheaper labeling costs

Intuitively, with cheaper labeling costs MCAL should use more human labeling to train the classifier. This in turn should enable a larger fraction of data to be labeled by the classifier. To validate this, we used the Satyam [26] labeling service that incurs a  $10\times$  lower labeling cost compared to Amazon’s labeling service. The effect of this reduction is most evident for CIFAR-100 in Table 2 as MCAL chooses to train the classifier using 57.6% of the data (instead of 32% using Amazon labeling service). This increases the classifier’s accuracy allowing it to label 20% of the dataset (instead of 10% using Amazon labeling service). For other datasets, the differences are less dramatic (they use 2.5-5% more data to train the classifier). For these datasets, there is no change in  $(|S|)/(|X|)$  because our resolution in this dimension is limited to 5% since we change  $\theta$  in increments of 5%.

Figures 10, 11, and 12 depict the effect of using various choices of  $\delta$  on overall cost for various classifiers and data sets using Satyam as the labeling service. As seen in these figures, the lower labeling cost alters the tradeoff curves. The figures also depict the corresponding MCAL cost as well as the human labeling cost for reference. As seen from these figures, MCAL achieves a lower overall cost compared to all these possible choices in this case as well.

## 6 Conclusions

Motivated by the emergence of labeling platforms such as Amazon Sagemaker [1] and Google Labeling Services [3], which incurs prohibitive human labeling cost, this paper asks: “How to label a data set at minimum cost”? To do this, it trains a classifier  $\mathcal{D}$  using a set  $B$  from the data set to label  $S$  samples, and uses humans to label the rest. The key challenge is to find the optimal value of  $B$  that minimizes total cost. MCAL first estimates  $|B|$  by modeling the accuracy vs. training set size as a truncated power-law, then uses active learning to find samples to include in  $B$  to minimize overall cost, of which training cost can be a significant component. The evaluation shows that it can achieve up to  $6\times$  lower cost than using humans to label the data set, and is always cheaper than using active learning with the lowest-cost batch size.



## References

- [1] Amazon sagemaker data labeling. <https://docs.aws.amazon.com/sagemaker/latest/dg/sms-data-labeling.html>. 1, 2, 6, 8
- [2] Figure eight data annotation platform. <https://www.figure-eight.com/>. 1, 2
- [3] Google ai platform data labeling service. <https://cloud.google.com/data-labeling/docs/>. 1, 2, 8
- [4] Keras Documentation: Training Resnet on CIFAR-10. [https://keras.io/examples/cifar10\\_resnet/](https://keras.io/examples/cifar10_resnet/). 6
- [5] Sara Beery, Grant Van Horn, and Pietro Perona. Recognition in terra incognita. In *The European Conference on Computer Vision (ECCV)*, September 2018. 3
- [6] William H. Beluch, Tim Genewein, Andreas Nürnberger, and Jan M. Köhler. The power of ensembles for active learning in image classification. In *The IEEE Conference on Computer Vision and Pattern Recognition (CVPR)*, June 2018. 3
- [7] Clemens-Alexander Brust, Christoph Käding, and Joachim Denzler. Active learning for deep object detection. *Proceedings of the 14th International Joint Conference on Computer Vision, Imaging and Computer Graphics Theory and Applications*, 2019. 3
- [8] Stephen M. Burroughs. *Upper-truncated power laws and self-similar criticality in geophysical processes*. PhD thesis, University of South Florida, July 2001. 3
- [9] Junghwan Cho, Kyewook Lee, Ellie Shin, Garry Choy, and Synho Do. How much data is needed to train a medical image deep learning system to achieve necessary high accuracy?, 2015. 3
- [10] Gabriella Contardo, Ludovic Denoyer, and Thierry Artieres. A meta-learning approach to one-step active learning, 2017. 3
- [11] Aron Culotta and Andrew McCallum. Reducing labeling effort for structured prediction tasks. volume 2, pages 746–751, 01 2005. 2
- [12] Ido Dagan and Sean P. Engelson. Committee-based sampling for training probabilistic classifiers. In *In Proceedings of the Twelfth International Conference on Machine Learning*, pages 150–157. Morgan Kaufmann, 1995. 2
- [13] Rosa Figueroa, Qing Zeng-Treitler, Sasikiran Kandula, and Long Ngo. Predicting sample size required for classification performance. *BMC medical informatics and decision making*, 12:8, 02 2012. 3
- [14] Kaiming He, Xiangyu Zhang, Shaoqing Ren, and Jian Sun. Deep residual learning for image recognition. In *Proceedings of the IEEE conference on computer vision and pattern recognition*, pages 770–778, 2016. 3, 6
- [15] Joel Hestness, Sharan Narang, Newsha Ardalani, Gregory Diamos, Heewoo Jun, Hassan Kianinejad, Md. Mostofa Ali Patwary, Yang Yang, and Yanqi Zhou. Deep learning scaling is predictable, empirically, 2017. 3
- [16] Peiyun Hu, Zack Lipton, Anima Anandkumar, and Deva Ramanan. Active learning with partial feedback. In *International Conference on Learning Representations*, 2019. 3
- [17] R. Istrate, F. Scheidegger, G. Mariani, D. Nikolopoulos, C. Bekas, and A. C. I. Malossi. Tapas: Train-less accuracy predictor for architecture search. *Proceedings of the AAAI Conference on Artificial Intelligence*, 33:3927–3934, Jul 2019. 3
- [18] Mark Johnson, Peter Anderson, Mark Dras, and Mark Steedman. Predicting accuracy on large datasets from smaller pilot data. In *Proceedings of the 56th Annual Meeting of the Association for Computational Linguistics (Volume 2: Short Papers)*, pages 450–455, Melbourne, Australia, July 2018. Association for Computational Linguistics. 3
- [19] Chieh-Chi Kao, Teng-Yok Lee, Pradeep Sen, and Ming-Yu Liu. *Localization-Aware Active Learning for Object Detection*, pages 506–522. 05 2019. 3
- [20] Aaron Klein, Stefan Falkner, Jost Tobias Springenberg, and Frank Hutter. Learning curve prediction with bayesian neural networks. In *ICLR*, 2017. 3
- [21] Ksenia Konyushkova, Raphael Sznitman, and Pascal Fua. Introducing geometry in active learning for image segmentation. 08 2015. 3

- [22] Ksenia Konyushkova, Raphael Sznitman, and Pascal Fua. Learning active learning from data. In I. Guyon, U. V. Luxburg, S. Bengio, H. Wallach, R. Fergus, S. Vishwanathan, and R. Garnett, editors, *Advances in Neural Information Processing Systems 30*, pages 4225–4235. Curran Associates, Inc., 2017. 3
- [23] Akshay Krishnamurthy, Alekh Agarwal, Tzu-Kuo Huang, Hal Daumé III, and John Langford. Active learning for cost-sensitive classification. *CoRR*, abs/1703.01014, 2017. 3
- [24] Alex Krizhevsky. Learning multiple layers of features from tiny images. Technical report, 2009. 2, 3, 6
- [25] Zhiyun Lu, Liyu Chen, Chao-Kai Chiang, and Fei Sha. Hyper-parameter tuning under a budget constraint. *Proceedings of the Twenty-Eighth International Joint Conference on Artificial Intelligence*, Aug 2019. 3
- [26] Hang Qiu, Krishna Chintalapudi, and Ramesh Govindan. Satyam: Democratizing groundtruth for machine vision. *arXiv preprint arXiv:1811.03621*, 2018. 6, 8
- [27] Vittorio Sala. Power law scaling of test error versus number of training images for deep convolutional neural networks. In *Proc. of SPIE*, volume 11059 of *Society of Photo-Optical Instrumentation Engineers (SPIE) Conference Series*, page 1105914, Jun 2019. 3
- [28] Ozan Sener and Silvio Savarese. Active learning for convolutional neural networks: A core-set approach, 2017. 3
- [29] Burr Settles. Active learning literature survey. Technical report, 2010. 2, 4, 6
- [30] Yanyao Shen, Hyokun Yun, Zachary Lipton, Yakov Kronrod, and Animashree Anandkumar. Deep active learning for named entity recognition. *Proceedings of the 2nd Workshop on Representation Learning for NLP*, 2017. 3
- [31] Keze Wang, Xiaopeng Yan, Dongyu Zhang, Lei Zhang, and Liang Lin. Towards human-machine cooperation: Self-supervised sample mining for object detection. *CoRR*, abs/1803.09867, 2018. 3
- [32] Keze Wang, Dongyu Zhang, Ya Li, Ruimao Zhang, and Liang Lin. Cost-effective active learning for deep image classification. *IEEE Transactions on Circuits and Systems for Video Technology*, 27(12):2591–2600, Dec 2017. 3
- [33] Han Xiao, Kashif Rasul, and Roland Vollgraf. Fashion-mnist: a novel image dataset for benchmarking machine learning algorithms, 2017. 2, 6
- [34] Lin Yang, Yizhe Zhang, Jianxu Chen, Siyuan Zhang, and Danny Z. Chen. Suggestive annotation: A deep active learning framework for biomedical image segmentation. *Lecture Notes in Computer Science*, page 399–407, 2017. 3

## 7 Appendix

### A Power-law and Truncated Power-law Fit

In this section, we show power law and truncated power law fitting results on all combinations of datasets and models. Figure 13, Figure 14, Figure 15 show fitting results on CIFAR-10, Figure 16, Figure 17, Figure 18 on CIFAR-100, and Figure 19, Figure 20, Figure 21 on Fashion. As an example, we show the fitting results on the error profile of  $\theta = 50\%$  in all figures in this section. In all combinations of datasets and models, while using more points gives higher accuracy and better prediction, both power-law and truncated power-law can get stable and precise prediction using a very limited number of small sample points.

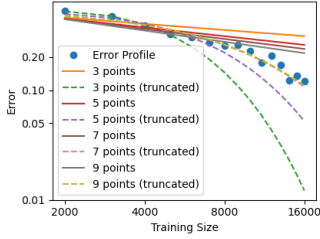


**Figure 13:** Power-law and Truncated Power-law fits on CIFAR-10 using CNN18

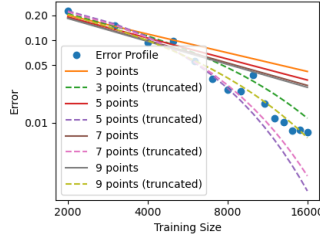


**Figure 14:** Power-law and Truncated Power-law fits on CIFAR-10 using RESNET18

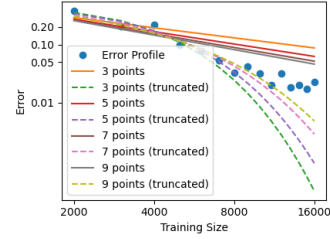


**Figure 15:** Power-law and Truncated Power-law fits on CIFAR-10 using RESNET50

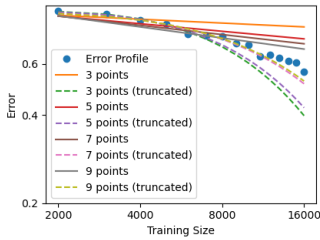


**Figure 16:** Power-law and Truncated Power-law fits on CIFAR-100 using CNN18

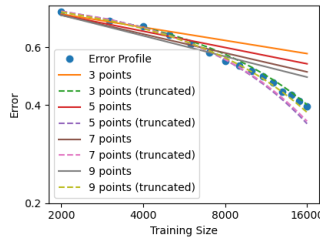


**Figure 17:** Power-law and Truncated Power-law fits on CIFAR-100 using RESNET18

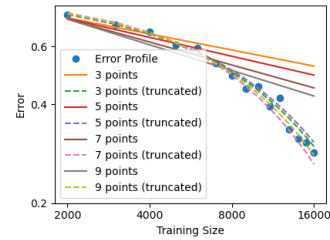


**Figure 18:** Power-law and Truncated Power-law fits on CIFAR-100 using RESNET50

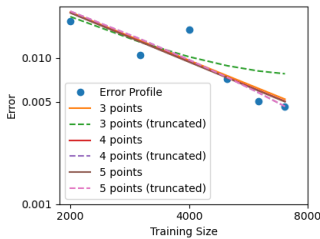


**Figure 19:** Power-law and Truncated Power-law fits on Fashion using CNN18

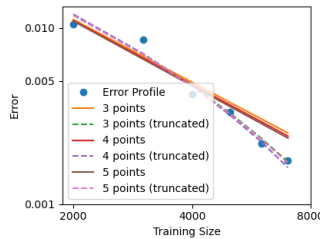


**Figure 20:** Power-law and Truncated Power-law fits on Fashion using RESNET18

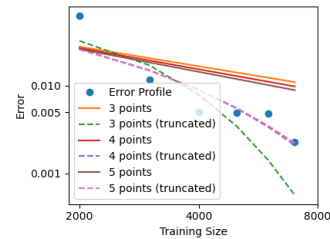


**Figure 21:** Power-law and Truncated Power-law fits on Fashion using RESNET50